Effect of Zn and Ni Impurities on the Quasiparticle Renormalization of Superconducting Bi-2212

V. B. Zabolotnyy,[1] S. V. Borisenko,[1] A. A. Kordyuk,[1,2] J. Fink,[1] J. Geck,[1] A. Koitzsch,[1] M. Knupfer,[1] B. Büchner,[1]
H. Berger,[3] A. Erb,[4] C. T. Lin,[5] B. Keimer,[5] and R. Follath[6]

[1]*Institute for Solid State Research, IFW-Dresden, P.O. Box 270116, D-01171 Dresden, Germany*
[2]*Institute of Metal Physics of National Academy of Sciences of Ukraine, 03142 Kyiv, Ukraine*
[3]*Institute of Physics of Complex Matter, EPFL, CH-1015 Lausanne, Switzerland*
[4]*Walther-Meißner-Institut, Bayerische Akademie der Wissenschaften, Walther-Meißner Strasse 8, 85748 Garching, Germany*
[5]*Max-Planck Institut für Festkörperforschung, D-70569 Stuttgart, Germany*
[6]*BESSY GmbH, Albert-Einstein-Strasse 15, 12489 Berlin, Germany*
(Received 23 August 2005; published 26 January 2006)

The Cu substitution by Zn and Ni impurities and its influence on the mass renormalization effects in angle-resolved photoelectron spectra (ARPES) of $Bi_2Sr_2CaCu_2O_{8-\delta}$ is addressed. We show that the nonmagnetic Zn atoms have a much stronger effect in both the nodal and antinodal parts of the Brillouin zone than magnetic Ni. The observed changes are consistent with the behavior of the spin resonance mode as seen by inelastic neutron scattering in YBCO. This strongly suggests that the ''peak-dip-hump'' and the kink in ARPES on the one side and neutron resonance on the other are closely related features.

The unique sensitivity of angle-resolved photoemission (ARPES) to the many-body effects in solids brings this technique to the forefront of modern research in the field of high-temperature superconductivity (HTSC). The anomalies in the single-particle spectral function of a superconductor, detected and well characterized along the high symmetry directions of the Brillouin zone (BZ), are commonly believed to be crucial for understanding HTSC. Along the BZ diagonal, the renormalization effects are represented by an unusual dispersion, the so-called ''kink'' [1–3]. In the vicinity of the $(\pi, 0)$ point of the BZ, where the order parameter reaches its maximum, the renormalization is noticeably stronger and makes itself evident even in the shape of a single spectral line measured for a fixed momentum [4–6].

It is widely accepted that coupling to a collective mode [7,8] naturally explains these anomalies. The origin of this mode remains a current controversy between the two most frequently proposed candidates: phonons and spin fluctuations.

Existing photoemission data suggest substantial dependence of the coupling between the electrons and the mode on momentum [2], hole doping [6,9], and temperature [5,10], which well fits the magnetic scenario. However, other similar ARPES experiments are interpreted in terms of phonons [11,12]. In order to resolve this controversy, one needs a way to vary separately either the phononic or the magnetic spectrum. Variation in the phononic spectrum can be achieved by the use of different isotopes. Such an experiment for HTSC has recently been reported [13], but its ''unusual'' character (all major effects have been observed at high energies, 100–300 meV) leaves the problem of low-energy anomalies, which are relevant for the superconductivity, unsolved. There is also a possibility to change the magnetic spectrum via doping different types

of impurities into the Cu-O plane. It is known from inelastic neutron scattering (INS) [14,15] that substitution of Zn and Ni leads to substantial changes in the imaginary part of spin susceptibility.

In this Letter, we show that substitution of Zn and Ni essentially influences the renormalization anomalies in ARPES spectra along both the nodal and antinodal regions of the BZ. Moreover, the changes in ARPES spectra are in good correspondence to those observed in magnetic spectra by INS. This provides evidence that it is the magnetic excitations that are responsible for the unusual renormalization features in the quasiparticle excitation spectrum of cuprates.

The ARPES experiments were carried out at the U125/1-PGM beam line with an angle-multiplexing photoemission spectrometer (SCIENTA SES100) at BESSY. Overall energy resolution was set to 20 meV, and angular resolution was 0.2°, which yields a wave vector resolution 0.013 and 0.009 $Å^{-1}$ for 50 and 27 eV excitation energies, respectively. All data were acquired at $T = 30$ K in the superconducting state for three high quality samples: nearly optimally doped pure BSCCO ($T_C = 92$ K), Zn substituted BSCCO with nominal Zn concentration close to 1% ($T_C = 86$ K), and 2% Ni substituted BSCCO ($T_C = 87$ K).

The two regions in the BZ that we focused on are schematically shown in Fig. 1(a). The fat black spot at $M(\pi, 0)$ corresponds to an antinodal energy distribution curve (EDC), which is a spectrum measured for a fixed momentum. In the nodal region, the set of k points for which the spectra were recorded is denoted by a double-headed arrow directed along the BZ diagonal.

First, we consider the antinodal region. In the general case, the EDC taken at the $(\pi, 0)$ point would consist of two peaks due to the bilayer split band [16,17]. It has been shown that the contribution from the bonding band can be
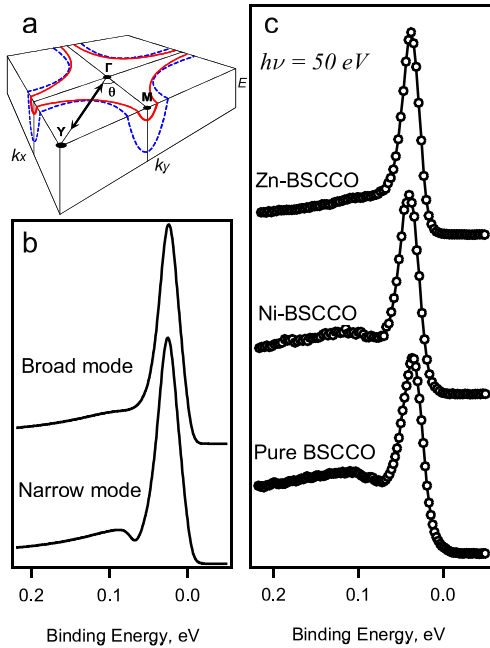
FIG. 1 (color online). (a) Cut of a $k\omega$ space at the Fermi level. The top of the cube contains two sheets of the Fermi surface; the red solid line corresponds to the dispersion of the antibonding band; the blue dashed one to the bonding band. (b) Model line shape of the $(\pi, 0)$ EDC, when coupled to a narrow (2 meV) and broad (20 meV) collective mode. (c) Experimental EDC's taken at the $(\pi, 0)$ point.

completely removed by a proper choice of excitation energy [17] (in this case, $h\nu = 50$ eV). Nevertheless, at least for the underdoped samples [18], the line shape is not reduced to a single peak and has a dip at a higher binding energy. The presence of the dip in a single band EDC is well explained in terms of coupling to a collective mode [7,8]. Such an interaction with a sharp mode with energy $\Omega_{\rm mode}$ leads to the increase of the scattering rate at binding energies higher than $\Omega_{\rm mode} + \Delta$, where Δ is a superconducting gap, i.e., to a steplike feature in the imaginary part of the self-energy and a logarithmic divergence in the real part of the self-energy giving rise to a dip in the photoemission line shape. When the mode has a finite width, the dip smears out as demonstrated in Fig. 1(b). Therefore, the dip can be a good indicator of the mode width and energy. Broadening of the mode described above well corresponds to our experimental data presented in Fig. 1(c). Comparing these EDC's, measured at the $(\pi, 0)$ point of the BZ with 50 eV photon energy, we see a striking difference in the line shapes caused by the impurity substitution: While for the pure sample the spectrum has a pronounced dip, for the Zn substituted sample the dip almost completely vanishes. For the Ni substituted sample, the dip "strength" is intermediate. The dip vanishing with Zn doping is a robust effect that we observed for numerous samples and was one of the reasons to conduct this systematic study.

Another change in the spectra that one can notice is an increase of the intensity of the low-energy peak relative to

the spectral weight at higher binding energies upon Ni substitution and an even stronger effect on Zn substitution. In a simple model where we explain the spectral weight at the $(\pi, 0)$ point by a strong coupling to a mode (e.g., the neutron resonance mode), such an intensity variation could be accounted for by a stronger coupling to the mode upon impurity substitution. A higher coupling to the mode would be related to a larger imaginary part of the self-energy, and this would cause a stronger broadening and, therefore, a reduction of the intensity in the "hump" region. On the other hand, such a broadening would also result in a flattening of the hump that we do not observe here. In addition, we do not see in the dispersion of the bonding band (not shown) any clear evidence for an increase of the mass enhancement with Zn doping. Thus, in order to account for all changes in the line shape, one needs a model that also takes into consideration the possible difference in elastic scattering contributions (e.g., due to different surface qualities) and different extrinsic backgrounds.

Now we turn to the spectra measured for the set of k points lying along the BZ diagonal. To avoid the complications of bilayer splitting at this part of the BZ, the following spectra were measured with $h\nu = 27$ eV, when again only one of the bilayer split bands is visible [19]. The raw distributions of photoemission intensity as a function of energy and momentum are presented in Figs. 2(a)–2(c). In the second row in Fig. 2, we show the
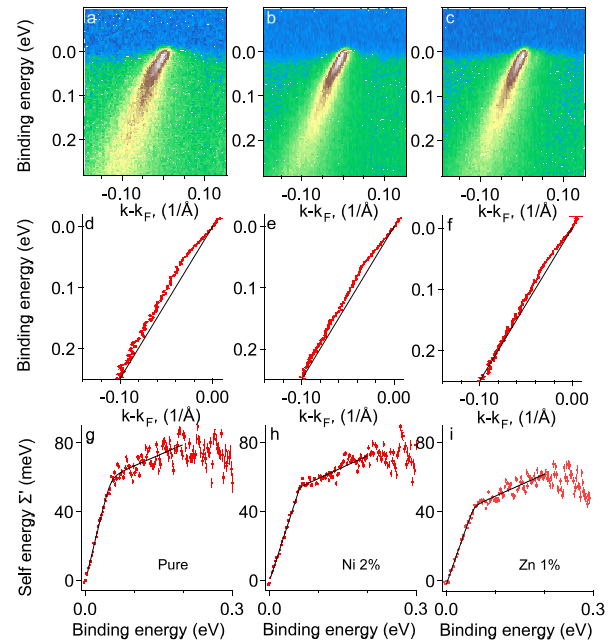

FIG. 2 (color online). (a)–(c) Photoemission intensity distributions along the BZ diagonal. (a) Pure BSCCO, (b) Ni substituted, and (c) Zn substituted BSCCO. The middle row shows corresponding experimental dispersion. In the last row, the real part of the self-energy obtained by subtractions of the bare band is displayed. The black solid lines are guides to eye, while the red symbols represent the data points.

experimental dispersion obtained from the maxima position of the Lorentzians that provide the best fit to the momentum dispersion curves [1]. The straightforward way to estimate a degree of the renormalization effects is to draw one and the same "guide" line from the Fermi level (FL) to some fixed point on the experimental dispersion curve and treat the area between the dispersion curve and the guide line as an effective measure of renormalization. It is easy to see that renormalization in the case of the Zn substituted sample is decreased in comparison to the pure sample. Subtracting a bare particle band dispersion from the experimental dispersion, the real part of the self-energy can be obtained. Here, as follows from a self-consistent Kramers-Krönig procedure [20], for the bare band dispersion we used a parabolic band with its bottom lying 0.8 eV below the FL. Defining a coupling constant as derivative of the real part of the self-energy at the FL, we find that $\lambda^{nod}_{pure} \approx 1.06$, $\lambda^{nod}_{Ni} \approx 0.88$, and, for the Zn doped sample, it has the lowest value $\lambda^{nod}_{Zn} \approx 0.76$. We note that, although the obtained absolute values for λ^{nod} depend on the parameters of the bare band dispersion, their ratio remains almost insensitive to the position of the bottom of the bare band, provided that the bare band is the same for all three samples. Therefore, it would be more accurate to say that the coupling constant for the nodal direction is reduced by approximately 15% for the 2% Ni doped sample and by 30% for 1% Zn doped sample as compared to the pure one. The fact that the Zn doped sample has nearly the same T_C as the Ni doped one, in spite of different λ^{nod}, is not surprising. Because of the strong anisotropy of the coupling, the critical temperature of a d-wave superconductor is not solely defined by λ^{nod}.

A link between the modifications in our spectra and changes in the spin fluctuation spectrum with impurity substitution was based on the implication that we have equal charge doping of the samples. It is known that the renormalization features are weakening with overdoping in both nodal and antinodal directions [6,9]. Therefore, different hole doping might be a possible explanation. In order to evaluate the hole doping level, we measured the FS maps in k space for all samples, which, in addition, allowed us to know precisely our position in the reciprocal space when measuring nodal and antinodal spectra. In a false color scale (Fig. 3), we show experimental data, which are the photoemission intensity distributions as a function of momentum recorded for a fixed energy, namely, 20 meV below the FL. Figures 3(a)–3(c) correspond to the samples under consideration, and, for comparison, in Fig. 3(d) we give the identical map for an overdoped sample with the hole doping δ within 0.19–0.20. Gray-scale images below the experimental data represent tight-binding fits to the antibonding sheets of the FS [21]. The area of antibonding sheets of the FS can be used as a good relative doping measure. We focus attention on the "lens" [Fig. 3(d)] formed by the shadow and the 1st order diffraction replica. Even from its size, which is determined by the size of the
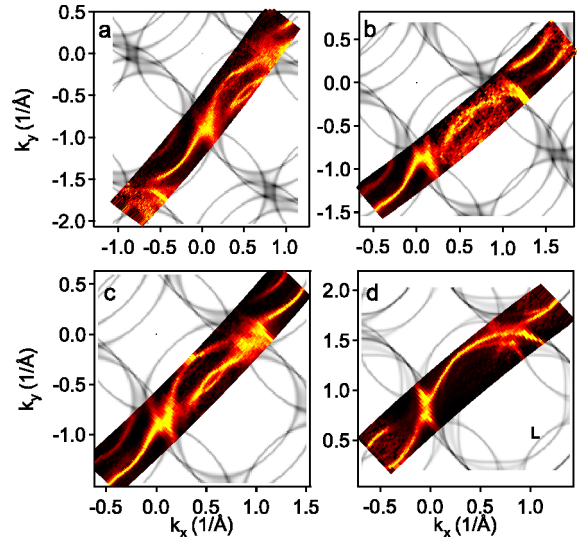

FIG. 3 (color online). Cuts of $k\omega$ space made 20 meV below the Fermi level and tight-binding fits. (a) Ni substituted sample. (b) Zn substituted sample. (c) Pure BSCCO close to optimal doping. (d) Overdoped BSCCO, $\delta \approx 0.20$; L denotes lens formed by the shadow band and the 1st order diffraction replica.

FS, it is clear that the first three samples have very close hole doping and that the doping of the fourth sample is notably higher. Quantitative evaluation gives the following result: $(S_a - 1/2):(S_b - 1/2):(S_c - 1/2):(S_d - 1/2) \approx 1.00:1.01:0.98:1.14$, where S_i denotes the ratio of the area of the occupied part of the BZ to the area of the whole BZ. The values for S_i were obtained from the tight-binding fit of the experimental map for each panel (a)–(d). However, a charge doping induced suppression of the renormalization features would require a deviation of the hole concentration of about 30% [6]. So we see that the difference in charge doping for our sample is negligible to account for the substantial change in the line shape [Fig. 1(c)] at the antinode, as well as for the different renormalization constants (Fig. 2) for the nodal spectra.

We find that our experimental observations of the dip smearing in the $(\pi, 0)$ EDC are in good agreement with the results of INS experiments. The comparison with INS is most pertinent here, since it gives a detailed insight into the changes of a spin fluctuation spectrum modified by the impurities and allows us to make a comparison with those that we see in ARPES spectra. The direct observation of the magnetic resonance mode by INS in YBCO demonstrates its strong sensitivity to impurities incorporated into Cu-O planes. When, for a pure sample, the mode is sharply peaked at ~40 meV with a FWHM being resolution limited [22], for 1% Zn substituted YBCO the mode attains a finite width of about 10 meV [14]. Gradual broadening of the resonance and decrease of its intensity is traced in detail in Ref. [15]. From Ref. [14] it follows that an introduction of 3% of Ni results in approximately the same intensity of the resonance at its peak as in the case of 1% Zn doping, supporting the idea that nonmagnetic Zn

has stronger influence on spin dynamics than Ni, which is the same that we see in ARPES spectra.

It is also worth mentioning that Raman scattering experiments on Zn and Ni substituted YBCO crystals show no apparent changes in the structure of phonon anomalies [23,24] at room temperature, suggesting that the lattice dynamics remains unchanged. Similar results, except for the peak at 340 cm^{-1}, are obtained in Ref. [25] for the superconducting state. This peak shows a small decrease of its intensity and insignificant, as compared to magnetic resonance mode, broadening from 1.6 to 1.9 meV. It is clear that such a broadening cannot account for the vanishing of the dip in the $(\pi, 0)$ spectra. Therefore, we conclude that the smearing of the dip in the $(\pi, 0)$ EDC with impurity doping is a straightforward consequence of the magnetic resonance mode broadening and possibly a decrease of its integral intensity.

For the nodal direction (BZ diagonal), the situation is more complicated. According to Ref. [26], the renormalization effects in nodal spectra are caused mainly by scattering of the electrons between nodes and a van Hove singularity in the density of states at the $(\pi, 0)$ point by the resonance mode centered at antiferromagnetic vector $Q(\pi, \pi)$. This serves as a good explanation for the fact that the renormalization effects are much weaker in the node than those in the vicinity of the $(\pi, 0)$ point. But it also means that the renormalization has to increase with the resonance mode broadening in momentum space when impurities are doped into the Cu-O plane [14]. On the contrary, our observations show that the dimensionless coupling constant λ decreases, suggesting that the scattering by the antiferromagnetic vector $Q(\pi, \pi)$ does not have the dominant contribution in the nodal spectra renormalization effects [27]. The new resonance feature in a magnetic excitation spectrum [28,29] peaked at an energy close to 54 meV, and an incommensurate vector $Q_{IC}^{*}(0.8\pi, 0.8\pi)$ provides scattering between the nodes and, therefore, should have a strong influence on the nodal spectra renormalization effects. The suppression of the new resonance, observed at 54 meV, with impurity doping is expected, since it belongs to the same dispersion curve [30]. However, its detailed evolution needs to be clarified, in order to put the problem into a quantitative domain.

In conclusion, we have shown that the substitution of Cu atoms in the Cu-O plane changes renormalization features in ARPES spectra in both nodal and antinodal parts of the Brillouin zone. The smearing of the dip in the antinodal EDC can be well explained by coupling of electrons to a magnetic resonance mode. The effect of Zn and Ni substitution on the antinodal ARPES spectra is in good agreement with the influence of these impurities on a magnetic resonance mode seen by INS experiments. These, in addition to the previous ARPES studies of temperature and doping dependence [2,6,9,19] of "peak-dip-hump" structure, mass renormalization near the antinodal region, and a kink in a nodal part of the Brillouin zone, provide another strong evidence that the mode, coupling to which causes observed renormalization effects, has a magnetic rather than phononic origin.

[1] T. Valla *et al.*, Science **285**, 2110 (1999).
[2] P. V. Bogdanov *et al.*, Phys. Rev. Lett. **85**, 2581 (2000).
[3] A. Kaminski *et al.*, Phys. Rev. Lett. **86**, 1070 (2001).
[4] M. R. Norman *et al.*, Phys. Rev. Lett. **79**, 3506 (1997).
[5] A. D. Gromko *et al.*, Phys. Rev. B **68**, 174520 (2003).
[6] T. K. Kim *et al.*, Phys. Rev. Lett. **91**, 167002 (2003).
[7] S. Engelsberg and J. R. Schrieffer, Phys. Rev. **131**, 993 (1963).
[8] A. W. Sandvik *et al.*, Phys. Rev. B **69**, 094523 (2004).
[9] P. D. Johnson *et al.*, Phys. Rev. Lett. **87**, 177007 (2001).
[10] A. A. Kordyuk *et al.*, Phys. Rev. Lett. **92**, 257006 (2004).
[11] T. Cuk *et al.*, Phys. Rev. Lett. **93**, 117003 (2004).
[12] T. P. Devereaux *et al.*, Phys. Rev. Lett. **93**, 117004 (2004).
[13] A. Lanzara *et al.*, Nature (London) **430**, 187 (2004).
[14] Y. Sidis *et al.*, Phys. Rev. Lett. **84**, 5900 (2000).
[15] Y. Sidis *et al.*, cond-mat/0006265.
[16] A. A. Kordyuk *et al.*, Phys. Rev. B **67**, 064504 (2003).
[17] A. A. Kordyuk *et al.*, Phys. Rev. Lett. **89**, 077003 (2002).
[18] S. V. Borisenko *et al.*, Phys. Rev. Lett. **90**, 207001 (2003).
[19] A. A. Kordyuk *et al.*, Phys. Rev. B **70**, 214525 (2004).
[20] A. A. Kordyuk *et al.*, Phys. Rev. B **71**, 214513 (2005).
[21] O. K. Andersen *et al.*, Phys. Chem. Solids **56**, 1573 (1995).
[22] H. F. Fong *et al.*, Phys. Rev. Lett. **75**, 316 (1995).
[23] N. Watanabe *et al.*, Phys. Rev. B **57**, 632 (1998).
[24] M. Käll *et al.*, Phys. Rev. B **53**, 3566 (1996).
[25] M. Limonov *et al.*, Phys. Rev. B **65**, 024515 (2002).
[26] M. Eschrig *et al.*, Phys. Rev. B **67**, 144503 (2003).
[27] A. V. Chubukov *et al.*, Phys. Rev. B **70**, 174505 (2004).
[28] S. Pailhes *et al.*, Phys. Rev. Lett. **93**, 167001 (2004).
[29] I. Eremin *et al.*, Phys. Rev. Lett. **94**, 147001 (2005).
[30] D. Reznik *et al.*, Phys. Rev. Lett. **93**, 207003 (2004).